

# Identification of the regions involved in DNA binding by the mouse PEBP2 $\alpha$ protein

Gabriela C. Pérez-Alvarado<sup>a</sup>, Audrey Munnerlyn<sup>b</sup>, H. Jane Dyson<sup>a</sup>, Rudolf Grosschedl<sup>b,c</sup>, Peter E. Wright<sup>a,\*</sup>

<sup>a</sup>Department of Molecular Biology and the Skaggs Institute for Chemical Biology, The Scripps Research Institute, 10550 N. Torrey Pines Road, La Jolla, CA 92037, USA

<sup>b</sup>Howard Hughes Medical Institute and Departments of Microbiology and Biochemistry, University of California, San Francisco, CA 94143, USA

<sup>c</sup>Gene Center and Institute of Biochemistry, University of Munich, 81377 Munich, Germany

Received 7 January 2000; received in revised form 18 February 2000

Edited by Thomas L. James

**Abstract** The polyomavirus enhancer binding protein 2 $\alpha$  (PEBP2 $\alpha$ ) is a DNA binding transcriptional regulatory protein that binds conserved sites in the polyomavirus enhancer, mammalian type C retroviral enhancers and T-cell receptor gene enhancers. Binding of PEBP2 $\alpha$  and homologous proteins to the consensus DNA sequence TGPYGGTPY is mediated through a protein domain known as the runt domain. Although recent NMR studies of DNA-bound forms of the runt domain have shown an immunoglobulin-like (Ig) fold, the identification of residues of the protein that are involved in DNA binding has been obscured by the low solubility of the runt domain. Constructs of the mouse PEBP2 $\alpha$ A1 gene were generated with N- and C-terminal extensions beyond the runt homology region. The construct containing residues Asp90 to Lys225 of the sequence (PEBP2 $\alpha$ 90–225) yielded soluble protein. The residues that participate in DNA binding were determined by comparing the NMR spectra of free and DNA-bound PEBP2 $\alpha$ 90–225. Analysis of the changes in the NMR spectra of the two forms of the protein by chemical shift deviation mapping allowed the unambiguous determination of the regions that are responsible for specific DNA recognition by PEBP2 $\alpha$ . Five regions in PEBP2 $\alpha$ 90–225 that are localized at one end of the  $\beta$ -barrel were found to interact with DNA, similar to the DNA binding interactions of other Ig fold proteins.

© 2000 Federation of European Biochemical Societies.

**Key words:** Polyoma virus enhancer binding protein 2 $\alpha$ ; Runt domain; Specific DNA binding; Conformational change; Nuclear magnetic resonance spectroscopy; Chemical shift deviation mapping

## 1. Introduction

The polyomavirus enhancer binding protein 2 (PEBP2), also termed core binding factor (CBF) or acute myeloid leukemia factor (AML), is a heteromeric DNA binding transcriptional regulatory protein [1]. It consists of a T-cell-specific  $\alpha$  subunit (PEBP2 $\alpha$ ) that mediates specific DNA recognition

and a ubiquitously expressed  $\beta$  subunit (PEBP2 $\beta$ ) that enhances DNA binding by the  $\alpha$  subunit [1]. PEBP2 $\alpha$  binds conserved sites in mammalian type C retroviral enhancers and the polyomavirus enhancer, contributing to the transcription of those viruses which utilize PEBP2 $\alpha$  for their own viral gene expression [2,3]. PEBP2 $\alpha$  also binds conserved sites in the enhancers of several genes specifically expressed in T cells, including the enhancers of T-cell receptor (TCR) chain genes  $\alpha$ ,  $\gamma$ ,  $\delta$  and  $\beta$ , as well as the immunoglobulin  $\mu$ -chain gene [2,4–6]. PEBP2 $\alpha$  is likely to be involved in tissue-specific transcriptional regulation in the T-lymphocyte lineage, since it is expressed throughout thymic T-cell development, rendering it a participant in lymphocyte development and hematopoiesis [7].

PEBP2 $\alpha$  consists of a highly conserved DNA binding domain known as the runt domain and a variable transactivation domain at the C-terminus [6]. The runt domains of PEBP2 $\alpha$  and homologous proteins bind to the consensus DNA sequence TGPYGGTPY [2,7]. Functional analysis and deletion studies of PEBP2 $\alpha$  cDNAs revealed that the runt domain includes the regions involved in both DNA binding and heterodimerization with the  $\beta$  subunit [1,8]. Runt domain proteins appear to bind DNA as monomers and can bind in the absence of their biological partner, PEBP2 $\beta$  [1].

In the mouse, there are three genes encoding the  $\alpha$  subunit of the PEBP2 $\alpha$  protein: PEBP2 $\alpha$ A/CBFA1/AML3, PEBP2 $\alpha$ B/CBFA2/AML1 and PEBP2 $\alpha$ C/CBFA3/AML2 [1,9,10]. Translocations at the C-terminus produce dominant-negative fusion proteins that can bind DNA strongly but do not activate transcription normally and are involved in several types of leukemia [11]. The AML1 (PEBP2 $\alpha$ B) gene is encoded on human chromosome 21 and is disrupted by the chromosomal translocation t(8;21)(q22;q22) associated with acute myeloid leukemia subtype M2 [12]. Disruption by the t(12;21)(p13;q22) translocation is found in 30% of childhood acute lymphoblastic leukemias (pre-B-cell) [13] and t(3;21)(q26;q22) is associated with therapy-related leukemias, myelodysplasia or blastic crisis of chronic myelogenous leukemia [14]. The biological importance of AML1 and AML3 was further shown by targeted gene inactivations that resulted in defects in hematopoiesis and bone formation, respectively [15,16].

In this paper, we characterize the secondary structural elements and topology of the runt domain of murine PEBP2 $\alpha$ A using NMR methods. We were able to study both the free and bound forms of the runt domain, allowing the unambiguous

\*Corresponding author. Fax: (1)-858-784 9822.  
E-mail: [wright@scripps.edu](mailto:wright@scripps.edu)

**Abbreviations:** PEBP2 $\alpha$ , polyoma virus enhancer binding protein 2 $\alpha$ ; AML1, acute myeloid leukemia 1; NMR, nuclear magnetic resonance; HSQC, heteronuclear single quantum coherence; NOESY, nuclear Overhauser effect spectroscopy; NOE, nuclear Overhauser effect; TOCSY, total correlation spectroscopy

identification of the regions that interact with DNA. Structural information on the PEBP2 $\alpha$  proteins has been limited until recently, when two solution structures of the runt domain of the PEBP2 $\alpha$ B gene (AML1, CBFA2) in the DNA-bound form were reported [17,18]. These studies reported difficulties in the unambiguous determination of the regions that bound DNA, due to the insolubility of the free form of the runt domain protein. The construct that we used for our studies was sufficiently soluble to allow for characterization of the free protein at low temperatures and high salt concentrations. We have therefore been able to determine the regions of the PEBP2 $\alpha$  runt domain involved in DNA binding from chemical shift deviation mapping combined with solution NMR structural studies.

## 2. Materials and methods

### 2.1. Preparation of protein samples

The gene sequence of the DNA binding runt domain of PEBP2 $\alpha$ A, corresponding to residues 90–225 of the mouse PEBP2 $\alpha$ A gene [1], was amplified using PCR methods and inserted between the *Nde*I and *Eco*RI restriction sites of the PET-21a(+) expression vector (Novagen). *Escherichia coli* BL21(DE3) cells harboring the vector, as well as the pUBS520 vector containing the *dnaY* gene (tRNA<sup>Arg</sup><sub>AGA/AGG</sub>), were grown at 25°C in minimal medium. Cells were induced with 1 mM isopropyl-1-thio- $\beta$ -D-galactopyranoside (IPTG) between 0.4 and 0.5 OD<sub>600</sub>. The cells were harvested after 11–12 h (<sup>15</sup>N and <sup>15</sup>N,<sup>13</sup>C uniformly isotopically labeled) and 35–42 h (<sup>2</sup>H,<sup>15</sup>N,<sup>13</sup>C uniformly isotopically labeled) when they reached OD<sub>600</sub> = 2. The cell pellet was resuspended in 50 mM Tris-HCl, pH 7, 0.1 M NaCl, 1 mM phenylmethylsulfonyl fluoride (PMSF), 2 mM ethylene diamine tetraacetic acid disodium salt (EDTA), 1% nonaethylene glycol octylphenyl ether (NP-40) and 100 mM dithiothreitol (DTT). The cells were lysed after sonication, centrifuged, and the supernatant containing the target protein was passed through a Hi-Trap Q column equilibrated in 34 mM Tris-HCl, pH 7, 20 mM K<sub>2</sub>SO<sub>4</sub> and 0.2%  $\beta$ -mercaptoethanol in order to remove any nucleic acids bound to the target protein. The flow through was loaded onto a Hi-Trap SP column (Pharmacia) equilibrated with the same buffer for FPLC purification. The target protein was eluted with increasing KCl concentration. The fractions containing the target protein were diluted and loaded onto a heparin-Sepharose column (Pharmacia) equilibrated in 34 mM Tris-HCl, pH 7, 20 mM K<sub>2</sub>SO<sub>4</sub>, 100 mM KCl and 0.2%  $\beta$ -mercaptoethanol and eluted with a KCl gradient. The eluted fractions were exchanged and concentrated using a Centrprep-3 (Amicon) in 20 mM Tris-HCl, pH 7, 20 mM K<sub>2</sub>SO<sub>4</sub>, 200 mM KCl and 0.2%  $\beta$ -mercaptoethanol. The protein was kept dilute and final purification was achieved in a Superdex-75 column (Pharmacia). Fractions were collected at the center of the peak and purity was assessed by analytical reverse-phase chromatography, Coomassie gradient SDS-PAGE gel electrophoresis (Bio-Rad), electrospray and MALDI mass spectroscopy. Pure fractions were concentrated to 0.2 mM and exchanged into the desired NMR buffer (20 mM Tris-HCl-d<sub>8</sub>, pH 7, 20 mM K<sub>2</sub>SO<sub>4</sub>, 100 mM KCl, 10 mM DTT and 5% D<sub>2</sub>O) using a NAP-25 column (Pharmacia).

### 2.2. DNA preparation

A DNA oligonucleotide (5'-CTCTGCGGTTAGGC-3') and its complementary strand, containing a high affinity recognition sequence [1,19], were obtained from Operon Technologies. Each single-stranded oligo was purified by reverse-phase HPLC on a C18 column. Fractions containing the pure oligos were lyophilized and resuspended in 200 mM KCl, pH 7 and detritylated by lowering the pH to 5.5 with 80% acetic acid. Detritylation was monitored by HPLC. After detritylation was completed, the DNA solutions were neutralized to pH 7 with KOH. Strands were annealed in stoichiometric amounts and the duplex DNA was purified via a Hi-Trap Q strong anion exchange column equilibrated in 200 mM KCl, pH 7 and eluted with increasing KCl concentrations. Pure fractions were combined, desalted and concentrated in a Centrprep-3 (Amicon) unit. The DNA duplex was characterized from its NMR spectra.

### 2.3. Preparation of the protein-DNA complex

Protein in the NMR buffer was titrated into concentrated DNA. Complex formation was monitored from the protein H<sup>N</sup> protons and nitrogen NH shifts in <sup>15</sup>N-HSQC spectra, as well as the shifts of the DNA imino protons (H<sup>N</sup>) in NOESY spectra. Upon reaching the 1:1 ratio, the complex was diluted with NMR complex buffer to remove salt that would interfere with the protein:DNA interaction and then exchanged into 20 mM Tris-HCl, pH 6.5, 20 mM K<sub>2</sub>SO<sub>4</sub>, 10 mM DTT, and 5% D<sub>2</sub>O and concentrated in a centrifugal concentrator (1 kDa molecular weight cut off, Filtron). The concentrated protein solution (350  $\mu$ M) was transferred to an NMR tube and flushed with Ar or N<sub>2</sub> gas.

### 2.4. NMR spectroscopy

All NMR spectra were recorded at 22°C and 32°C on Bruker 500 MHz AMX-II, 600 MHz DRX-Avance and 800 MHz DRX-Avance spectrometers equipped with triple-axis shielded gradient triple-resonance probes. NMR studies required <sup>15</sup>N,<sup>15</sup>N,<sup>13</sup>C and <sup>2</sup>H,<sup>15</sup>N,<sup>13</sup>C isotopically labeled recombinant PEBP2 $\alpha$ 90–225. Triple-labeled PEBP2 $\alpha$ 90–225 was 85% deuterated. NMR data processing was performed using Felix97 (Molecular Simulations, San Diego, CA), NMRPipe and NMRDraw [20]. Data were analyzed using the NMRview software [21]. Backbone resonances of PEBP2 $\alpha$ 90–225 were assigned sequence-specifically from 3D CT-HNCA, CT-HN(CO)CA, HN(CA)CB, HN(CO)CACB, HN(CO), HN(CA)CO triple resonance data [22–25], in combination with 3D <sup>15</sup>N-NOESY-HSQC, <sup>15</sup>N-TOCSY-HSQC and <sup>15</sup>N-HSQC-NOESY-HSQC [26] spectra. 3D <sup>15</sup>N-edited NOESY-HSQC ( $\tau_m$  = 125 ms) and <sup>13</sup>C-edited HMQC-NOESY ( $\tau_m$  = 100 ms) spectra were recorded in order to confirm resonance assignments and also to obtain structural information [22]. Secondary structural elements and topology were determined from a combination of secondary chemical shift analysis and identification of unambiguous NOEs [22,27,28].

### 2.5. Chemical shift analysis

Secondary shifts were calculated using published random coil values for H <sup>$\alpha$</sup> , C <sup>$\alpha$</sup> , C <sup>$\beta$</sup>  and C' nuclei [29] for the PEBP2 $\alpha$ 90–225:DNA complex. <sup>1</sup>H, <sup>15</sup>N and <sup>13</sup>C resonances were referenced relative to 2,2-dimethyl-2-silapentane-5-sulfonate, sodium salt (0 ppm). Appropriate corrections to the random coil shifts were made for residues preceding a proline residue [30] and for carbon nuclei attached to deuterium [31].

## 3. Results

### 3.1. Design of protein and DNA constructs

The initial construct encoding mainly the runt homology region of the murine PEBP2 $\alpha$ A1 protein (Val95–Lys225) proved to be highly insoluble and unsuitable for NMR studies. Several N-terminal and C-terminal extensions beyond the runt homology region were engineered by PCR methods and tested for solubility. One of them, which corresponds to residues Asp90–Lys225 (PEBP2 $\alpha$ 90–225), proved to be moderately soluble at NMR concentrations.

### 3.2. NMR resonance assignments of PEBP2 $\alpha$ 90–225

<sup>1</sup>H,<sup>15</sup>N-correlated NMR spectra of free PEBP2 $\alpha$ 90–225 showed signals characteristic of a folded protein plus sharp overlapped resonances indicative of flexible regions. Data collected on the free form of the protein were incomplete, with 25% of the signals missing due to broadening arising from conformational exchange on an intermediate time scale. The free protein was unstable at high concentrations, room temperature, low pH and low salt content. Nevertheless, we were able to make extensive backbone resonance assignments of free PEBP2 $\alpha$ 90–225 using 3D HNCA, HN(CA)CB and <sup>15</sup>N NOESY spectra. Upon DNA binding, many of the resonances that were in intermediate exchange appeared and other resonances were shifted, consistent with stabilization or structural

rearrangement of the regions involved in DNA binding (Fig. 1).

### 3.3. NMR resonance assignments of PEBP2 $\alpha$ 90–225 bound to a DNA duplex

The  $^1\text{H}$ ,  $^{15}\text{N}$ -HSQC spectrum of PEBP2 $\alpha$ 90–225 is well dispersed when it is complexed to DNA, indicating a unique folded conformation. Almost complete backbone resonance assignments were made. No amide proton NMR signals were assigned for backbone amide protons of residues N-terminal Met, Asp90, Arg123–Cys124, Gly184–Lys187, His206–Ile209 and Thr212–Gly216; these signals were broadened due to intermediate exchange. For the remaining residues, sequential connectivities were observed in the  $^{15}\text{N}$ -edited NOESY data and the triple resonance data. Although chemical shift dispersion of the majority of the backbone  $\text{H}^{\text{N}}$  protons is good, signal degeneracies were observed for many of the loop regions as well as some of the extended regions. Some of the signals affected upon binding to DNA were in conformational exchange and too broad to be fully characterized. At low temperature, the complex appeared to be unstable, and resonances of the free form of the protein and the DNA

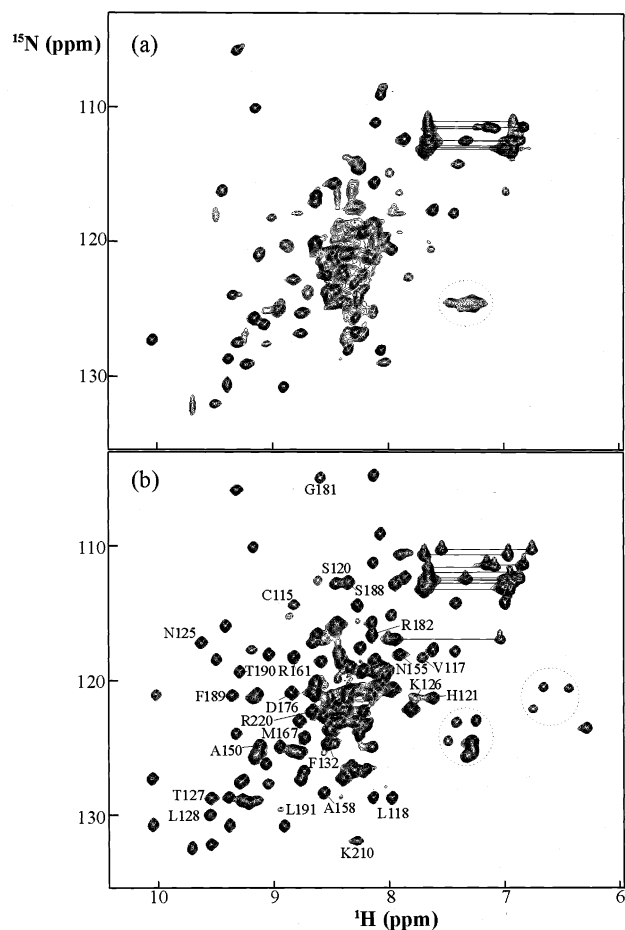


Fig. 1.  $^1\text{H}$ ,  $^{15}\text{N}$ -HSQC spectra recorded at 800 MHz under conditions described in the text of (a) free PEBP2 $\alpha$ 90–225 and (b) PEBP2 $\alpha$ 90–225 bound to DNA. Some of the resonances that are significantly shifted upon complexation with DNA are labeled. Arginine side chain resonances are encircled.

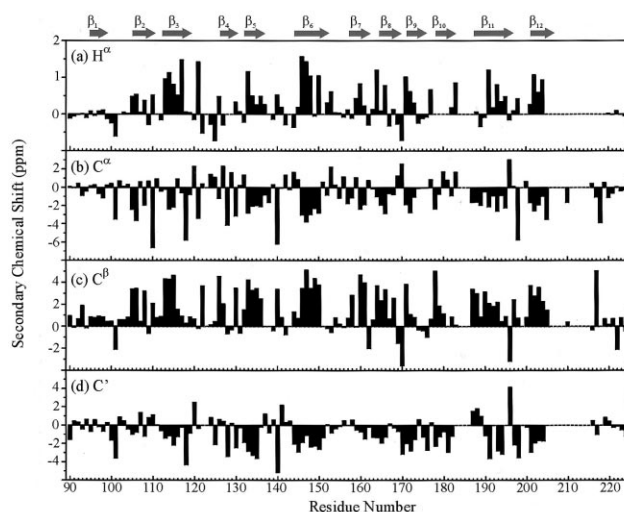


Fig. 2. Secondary chemical shifts plotted for (a)  $\text{H}^{\alpha}$ , (b)  $\text{C}^{\alpha}$ , (c)  $\text{C}^{\beta}$  and (d)  $\text{C}'$  nuclei of the PEBP2 $\alpha$ 90–225:DNA complex. The cartoon on top of the figure depicts the location of the  $\beta$ -strands in the runt domain.

duplex dominated the spectrum, with the signals of the complexed form being extremely broad. Data were collected at two temperatures, 22°C and 32°C, in order to assign resonances that were in the NMR intermediate time scale and overlapped. Data could not be collected at higher temperatures due to rapid precipitation of the sample.

### 3.4. Secondary structure determination

Elements of secondary structure were identified on the basis of the secondary chemical shifts of the  $\text{H}^{\alpha}$ ,  $\text{C}^{\alpha}$ ,  $\text{C}^{\beta}$ ,  $\text{C}'$  nuclei (Fig. 2). This information combined with the results from the  $^{15}\text{N}$ -NOESY-HSQC,  $^{15}\text{N}$ -HSQC-NOESY-HSQC and  $^{13}\text{C}$ -HMQC-NOESY spectra allowed determination of the topology of PEBP2 $\alpha$ 90–225. The secondary chemical shift of a particular nucleus is defined as the difference between the observed chemical shift and its random coil value. Theoretical calculations and empirical correlations have established that the secondary chemical shifts of certain backbone nuclei are largely determined by the local ( $\phi, \psi$ ) dihedral angles. This approach has been found to be extremely useful for identifying secondary structural elements of folded proteins and peptides [29]. The secondary shifts for the  $\text{H}^{\alpha}$ ,  $\text{C}^{\alpha}$ ,  $\text{C}^{\beta}$ ,  $\text{C}'$  of the assigned signals in PEBP2 $\alpha$ 90–225, together with NOE information from the  $^{15}\text{N}$ -edited NOESY, allowed the identification of  $\beta$ -strands, loops and turns for the secondary structure of PEBP2 $\alpha$ 90–225 (Fig. 2). From the NOE data, it was possible to define the topology of the  $\beta$ -sheets in the core. The runt domain in PEBP2 $\alpha$ 90–225 consists of at least 12  $\beta$ -strands that we define as:  $\beta_1$ (Val95–Ile98),  $\beta_2$ (Leu105–Ser110),  $\beta_3$ (Asn112–Leu118),  $\beta_4$ (Lys126–Leu128),  $\beta_5$ (Phe132–Ala136),  $\beta_6$ (Thr144–Gly151),  $\beta_7$ (Ser157–Arg161),  $\beta_8$ (Ser164–Lys168),  $\beta_9$ (Val171–Phe174),  $\beta_{10}$ (Arg178–Gly181),  $\beta_{11}$ (Lys187–Val195),  $\beta_{12}$ (Gln201–Tyr205). Of these strands, eight are arranged in a classical Greek key  $\beta$ -barrel [32] (Fig. 3). There are three  $\beta$ -hairpin connections, two tight turns,  $T_1$ (Ser110–Asn112) and  $T_2$ (Lys168–Gln170) and a longer connection  $T_3$ (Phe196–Pro200) containing two Pro resi-

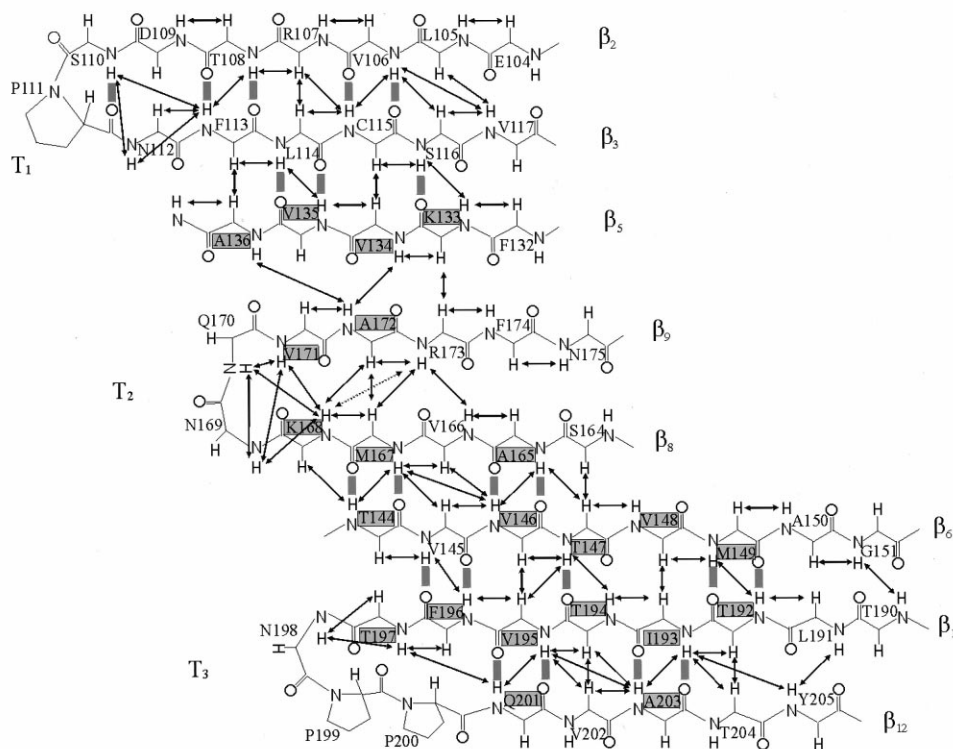


Fig. 3. Summary of some of the backbone NOE connectivities that define the topology of the  $\beta$ -sheets in PEBP2 $\alpha$ 90–225. Residues surrounded by rectangles indicate slow  $H^N$  exchange.

dues (Fig. 3). The topology of the Greek key motif was determined from the NOEs across the  $\beta$ -strands, as well as the NOEs that defined the tight  $\beta$ -turns. A summary of the NOE connectivities that determine the topology of the  $\beta$ -strands of PEBP2 $\alpha$ 90–225 is given in Fig. 3.

### 3.5. Mapping of residues involved in DNA binding

The regions in PEBP2 $\alpha$ 90–225 that are influenced by DNA binding were determined from changes in the backbone amide proton  $H^N$  and  $^{15}N$  chemical shifts upon binding to DNA (Fig. 4). The deviation in the chemical shift upon binding was evaluated using the formula:  $\Delta_{av} = \sqrt{(\Delta_H)^2 + (\Delta_N/5)^2}$ , where chemical shift changes between free and bound forms of the protein are represented by  $\Delta_H$  for the amide protons and  $\Delta_N$  for the amide nitrogens [33]. The chemical shifts of the backbone amide resonances remain unchanged for a large portion of the residues in PEBP2 $\alpha$ 90–225. Chemical shift differences above a threshold value ( $\Delta\delta > 0.07$  ppm) are apparent for about 40% of the resonances, which correspond to residues in five main regions within PEBP2 $\alpha$ 90–225. Shifts in these regions are consistent with mutagenesis data in which DNA binding is affected. The major changes in chemical shift correspond to residues Arg92, Val95–Glu96, Ile98–Ala99, His101, Glu104, Cys115, Val117–Leu118, His121–Trp122, Asn125–Lys126, Ala131–Val134, Ala150–Asn152, Tyr156, Ala158, Arg173–Phe174, Asp176–Leu177, Arg182, Phe189, Val211, Arg220–Arg223 and Lys225. Resonances of Ser120, Thr127, Leu128, Glu154–Asn155, Ser157, Glu159, Arg161, Arg178, Val180–Gly181, Ser183, Ser188, Thr190–Leu191 and Lys210 (marked with \* in Fig. 4) were not present in the data of free PEBP2 $\alpha$ 90–225 and appeared upon complex formation with DNA.

## 4. Discussion

The  $\beta$ -strand topology of PEBP2 $\alpha$ 90–225 contains a Greek key motif formed by strands  $\beta_3$ ,  $\beta_5$ ,  $\beta_9$ ,  $\beta_8$  and  $\beta_6$ . The topology of the strands resembles that of Cu,Zn-superoxide dismutase subunit (SOD) [34] and the immunoglobulin s-type and c-type chains [35]. Immunoglobulin-like folds are present in a diverse family of structures with no shared sequence

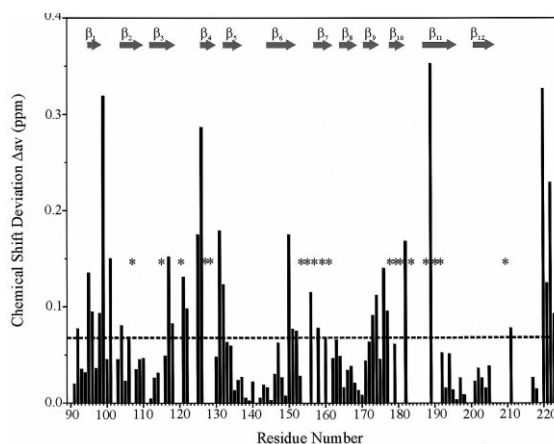


Fig. 4. Chemical shift deviations between free PEBP2 $\alpha$ 90–225 and PEBP2 $\alpha$ 90–225 bound to 5'-CTCTGCGGTTAGGC-3' plotted by residue. The dashed line in the graph corresponds to the threshold deviation (0.07 ppm). The asterisks indicate residues for which NH cross-peaks were not observed in the free form of the protein. The cartoon on top of the figure depicts the secondary structural elements in the DNA binding domain. No values are reported for residues 102, 111, 119, 129, 141, 199, 200, 216 and 219, which are prolines.

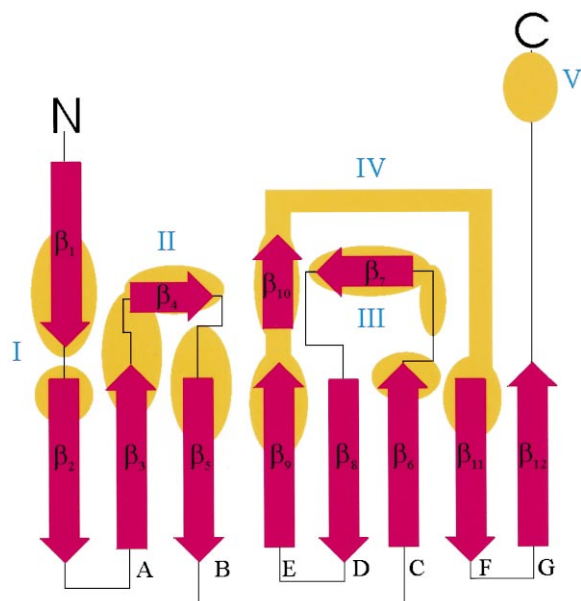


Fig. 5. Cartoon showing the topology of PEBP2 $\alpha$ 90–225 and adjacent  $\beta$ -strands (magenta). The figure denotes the regions affected upon contact with the DNA (yellow). The secondary structural elements are not drawn to scale. The main regions that are perturbed upon DNA binding are regions marked I–V (see text).

homology or function. The runt homology region does not present primary sequence homology with any other proteins out of the immediate runt family. The topology of PEBP2 $\alpha$ 90–225 resembles mostly that of Cu,Zn-SOD as defined by its hydrogen bond pattern deduced from the NOE data (Fig. 5) [36]. The reported structures of the runt domain of CBFA2 or AML1 defined a  $\beta$ -sheet topology similar to that of the immunoglobulin s-type fold composed of seven  $\beta$ -strands [17,18]. From our data, we defined a  $\beta$ -sheet topology composed of eight strands, which similarly to SOD are within hydrogen bonding distance of each other (Fig. 5).

The resonances of PEBP2 $\alpha$ 90–225 that are perturbed by DNA binding are mainly from residues in loops at one end of the molecule; resonances in the core  $\beta$ -sheets are relatively unaffected by DNA binding (Fig. 4). The chemical shift changes probably reflect direct contacts with the DNA or local conformational changes associated with DNA interactions. The largest chemical shift perturbations occur in five regions, as shown in Fig. 5. It is notable that mutations known to modulate DNA binding are all localized in the regions implicated in DNA contact by the chemical shift perturbations. Region I at the N-terminus (residues Val95–Val106) and region V at the C-terminus (residues Arg220–Lys225) (Fig. 5) do not form part of the core, but are still within the runt homology region. Interestingly, these regions are sensitive *in vivo* to mutations and deletions that modulate binding of PEBP2 $\alpha$  to DNA [37–39].

Region II (residues Cys115–Val134) shows major chemical shift deviations upon DNA binding. Site-directed mutagenesis or oxidation of the highly conserved Cys115 is detrimental to DNA binding activity [40,41]. Another cysteine within this region, Cys124, is not fully conserved among the different runt domain sequences and is replaced by a Ser in the *Drosophila* gene products. The Cys124Ser mutation enhances DNA binding, while the Cys124Asp substitution is deleterious

[41]. Werner and coworkers observed intermolecular NOEs to DNA from Val117 and Arg123, but not from any other residues, confirming that region II makes direct contact with the DNA and supporting our chemical shift mapping experiments. In region III (Ala150–Ala163), the Ala150Thr mutation diminishes DNA binding activity [42]. Mutations within region IV (residues Arg173–Thr192) have also proven to be detrimental to DNA binding (residues Arg173, Arg178, Ser183, Lys187, Phe189) [37,38,43,44].

The identification of the five regions in PEBP2 $\alpha$ 90–225 that participate in DNA recognition provides insights into the structural basis by which mutations in these regions affect DNA binding. All of these regions are localized at one end of the  $\beta$ -barrel in PEBP2 $\alpha$ , as in other Ig folds that interact with DNA (the N-terminal domain of the Rel homology region of NF- $\kappa$ B, the core domain of the p53 tumor suppressor and STAT-1 [45–47]). It has been suggested that the runt domain interacts with DNA at both ends of the  $\beta$ -barrel [18], but our results do not support these suggestions.

**Acknowledgements:** We gratefully acknowledge Dr. Brian M. Lee, Dr. Gerard Kroon, Linda Tennant and Dr. John Chung for technical assistance. We thank Drs. Ishwar Radhakrishnan, Maria Martínez-Yamout, Richard Kriwacki, Danilo Casimiro, John Love and Annette Atkins for valuable discussions. We thank Dr. Chris Kingsley for providing us with plasmids with the runt domain gene. This work was supported by grants from the National Institutes of Health and the Skaggs Institute for Chemical Biology (P.E.W.). G.C.P.A. acknowledges support from the Leukemia Society of America.

## References

- [1] Ogawa, E., Maruyama, M., Kagoshima, H., Inuzuka, M., Lu, J., Satake, M., Shigesada, K. and Ito, Y. (1993) Proc. Natl. Acad. Sci. USA 90, 6859–6863.
- [2] Wang, S. and Speck, N.A. (1992) Mol. Cell. Biol. 12, 89–102.
- [3] Thornell, A., Hallberg, B. and Grundstrom, T. (1991) J. Virol. 65, 42–50.
- [4] Prosser, H.M., Wotton, D., Gegonne, A., Ghysdael, J., Wang, S., Speck, N.A. and Owen, M.J. (1992) Proc. Natl. Acad. Sci. USA 89, 9934–9938.
- [5] Redondo, J.M., Pfohl, J.L., Hernandez-Munain, C., Wang, S., Speck, N.A. and Krangel, M.S. (1992) Mol. Cell. Biol. 12, 4817–4823.
- [6] Bae, S.C., Ogawa, E., Maruyama, M., Oka, H., Satake, M., Shigesada, K., Jenkins, N.A., Gilbert, D.J., Copeland, N.G. and Ito, Y. (1994) Mol. Cell. Biol. 14, 3242–3252.
- [7] Satake, M., Nomura, S., Yamaguchi-Iwai, Y., Takahama, Y., Hashimoto, Y., Niki, M., Kitamura, Y. and Ito, Y. (1995) Mol. Cell. Biol. 15, 1662–1670.
- [8] Giese, K., Kingsley, C., Kirshner, J.R. and Grosschedl, R. (1995) Genes Dev. 9, 995–1008.
- [9] Bae, S.-C., Takahashi, E., Zhang, Y.W., Ogawa, E., Shigesada, K., Namba, Y., Satake, M. and Ito, Y. (1995) Gene 159, 245–248.
- [10] Levanon, D., Negreanu, V., Bernstein, Y., Bar-Am, I., Avivi, L. and Groner, Y. (1994) Genomics 23, 425–432.
- [11] Speck, N.A., Stacey, T., Wang, Q., North, T., Gu, T.L., Miller, J., Binder, M. and Marin-Padilla, M. (1999) Cancer Res. 59, 1789s–1793s.
- [12] Miyoshi, H., Shimizu, K., Kozu, T., Maseki, N., Kaneko, Y. and Ohki, M. (1991) Proc. Natl. Acad. Sci. USA 88, 10431–10434.
- [13] Hiebert, S.W., Sun, W., Davis, J.N., Golub, T., Shurtleff, S., Buijs, A., Downing, J.R., Grosveld, G., Rousell, M.F., Gilliland, D.G., Lenny, N. and Meyers, S. (1996) Mol. Cell. Biol. 16, 1349–1355.
- [14] Nucifora, G., Begy, C.R., Erickson, P., Drabkin, H.A. and Rowley, J.D. (1993) Proc. Natl. Acad. Sci. USA 90, 7784–7788.
- [15] Okuda, T., van Deursen, J., Hiebert, S.W., Grosveld, G. and Downing, J.R. (1996) Cell 84, 321–330.

- [16] Otto, F., Thornell, A.P., Crompton, T., Denzel, A., Gilmour, K.C., Rosewell, I.R., Stamp, G.W., Beddington, R.S., Mundlos, S., Olsen, B.R., Selby, P.B. and Owen, M.J. (1997) *Cell* 89, 765–771.
- [17] Nagata, T., Gupta, V., Sorce, D., Kim, W.Y., Sali, A., Chait, B.T., Shigesada, K., Ito, Y. and Werner, M.H. (1999) *Nature Struct. Biol.* 6, 615–619.
- [18] Berardi, M.J., Sun, C.H., Zehr, M., Abildgaard, F., Peng, J., Speck, N.A. and Bushweller, J.H. (1999) *Struct. Fold. Des.* 7, 1247–1256.
- [19] Melnikova, I.N., Crute, B.E., Wang, S. and Speck, N.A. (1993) *J. Virol.* 67, 2408–2411.
- [20] Delaglio, F., Grzesiek, S., Vuister, G.W., Guang, Z., Pfeifer, J. and Bax, A. (1995) *J. Biomol. NMR* 6, 277–293.
- [21] Johnson, B.A. and Blevins, R.A. (1994) *J. Chem. Phys.* 29, 1012–1014.
- [22] Bax, A. and Grzesiek, S. (1993) *Acc. Chem. Res.* 26, 131–138.
- [23] Yamazaki, T., Lee, W., Revington, M., Mattiello, D.L., Dahlquist, F.W., Arrowsmith, C.H. and Kay, L.E. (1994) *J. Am. Chem. Soc.* 116, 6464–6465.
- [24] Yamazaki, T., Lee, W., Arrowsmith, C.H., Muhandiram, D.R. and Kay, L.E. (1994) *J. Am. Chem. Soc.* 116, 11655–11666.
- [25] Shan, X., Gardner, K.H., Muhandiram, D.R., Rao, N.S., Arrowsmith, C.H. and Kay, L.E. (1996) *J. Am. Chem. Soc.* 118, 6570–6579.
- [26] Zhang, O., Forman-Kay, J.D., Shortle, D. and Kay, L.E. (1997) *J. Biomol. NMR* 9, 181–200.
- [27] Wüthrich, K. (1986) *NMR of Proteins and Nucleic Acids*, John Wiley and Sons, New York.
- [28] Clore, G.M. and Gronenborn, A.M. (1994) *Methods Enzymol.* 239, 349–363.
- [29] Wishart, D.S. and Sykes, B.D. (1994) *Methods Enzymol.* 239, 363–392.
- [30] Wishart, D.S., Bigam, C.G., Holm, A., Hodges, R.S. and Sykes, B.D. (1995) *J. Biomol. NMR* 5, 67–81.
- [31] Gardner, K.H., Rosen, M.K. and Kay, L.E. (1997) *Biochemistry* 36, 1389–1401.
- [32] Richardson, J.S. (1977) *Nature* 268, 495–500.
- [33] Grzesiek, S., Stahl, S.J., Wingfield, P.T. and Bax, A. (1996) *Biochemistry* 35, 10256–10261.
- [34] Tainer, J.A., Getzoff, E.D., Beem, K.M., Richardson, J.S. and Richardson, D.C. (1982) *J. Mol. Biol.* 160, 181–217.
- [35] Bork, P., Holm, L. and Sander, C. (1994) *J. Mol. Biol.* 242, 309–320.
- [36] Richardson, J.S., Richardson, D.C., Thomas, K.A., Silverton, E.W. and Davies, D.R. (1976) *J. Mol. Biol.* 102, 221–235.
- [37] Lenny, N., Meyers, S. and Hiebert, S.W. (1995) *Oncogene* 11, 1761–1769.
- [38] Akamatsu, Y., Tsukumo, S., Kagoshima, H., Tsurushita, N. and Shigesada, K. (1997) *Gene* 185, 111–117.
- [39] Meyers, S., Downing, J.R. and Hiebert, S.W. (1993) *Mol. Cell. Biol.* 13, 6336–6345.
- [40] Kurokawa, M., Tanaka, T., Tanaka, K., Hirano, N., Ogawa, S., Mitani, K., Yazaki, Y. and Hirai, H. (1996) *J. Biol. Chem.* 271, 16870–16876.
- [41] Kagoshima, H., Akamatsu, Y., Ito, Y. and Shigesada, K. (1996) *J. Biol. Chem.* 271, 33074–33082.
- [42] Akamatsu, Y., Ohno, T., Hirota, K., Kagoshima, H., Yodoi, J. and Shigesada, K. (1997) *J. Biol. Chem.* 272, 14497–14500.
- [43] Lee, B., Thirunavukkarasu, K., Zhou, L., Pastore, L., Baldini, A., Hecht, J., Geoffroy, V., Ducy, P. and Karsenty, G. (1997) *Nature Genet.* 16, 307–310.
- [44] Levanon, D., Eisenstein, M. and Groner, Y. (1998) *J. Mol. Biol.* 277, 509–512.
- [45] Müller, C.W., Rey, F.A., Sodeoka, M., Verdine, G.L. and Harrison, S.C. (1995) *Nature* 373, 311–317.
- [46] Cho, Y., Gorina, S., Jeffrey, P.D. and Pavletich, N.P. (1994) *Science* 265, 346–355.
- [47] Chen, X.M., Vinkemeier, U., Zhao, Y.X., Jeruzalmi, D., Darnell Jr., J.E. and Kuriyan, J. (1998) *Cell* 93, 827–839.